

The DNA sequence and comparative analysis of human chromosome 10

P. Deloukas¹, M. E. Earthrowl¹, D. V. Grafham¹, M. Rubenfield^{2,3}, L. French¹, C. A. Steward¹, S. K. Sims¹, M. C. Jones¹, S. Searle¹, C. Scott¹, K. Howe¹, S. E. Hunt¹, T. D. Andrews¹, J. G. R. Gilbert¹, D. Swarbreck¹, J. L. Ashurst¹, A. Taylor¹, J. Battles², C. P. Bird¹, R. Ainscough¹, J. P. Almeida¹, R. I. S. Ashwell¹, K. D. Ambrose¹, A. K. Babbage¹, C. L. Bagguley¹, J. Bailey¹, R. Banerjee¹, K. Bates¹, H. Beasley¹, S. Bray-Allen¹, A. J. Brown¹, J. Y. Brown¹, D. C. Burford¹, W. Burrill¹, J. Burton¹, P. Cahill², D. Camire², N. P. Carter¹, J. C. Chapman¹, S. Y. Clark¹, G. Clarke¹, C. M. Clee¹, S. Clegg¹, N. Corby¹, A. Coulson¹, P. Dhami¹, I. Dutta¹, M. Dunn¹, L. Faulkner¹, A. Frankish¹, J. A. Frankland¹, P. Garner¹, J. Garnett¹, S. Gribble¹, C. Griffiths¹, R. Grocock¹, E. Gustafson^{2,3}, S. Hammond¹, J. L. Harley¹, E. Hart¹, P. D. Heath¹, T. P. Ho², B. Hopkins¹, J. Horne², P. J. Howden¹, E. Huckle¹, C. Hynds², C. Johnson¹, D. Johnson¹, A. Kana², M. Kay¹, A. M. Kimberley¹, J. K. Kershaw¹, M. Kokkinaki⁴, G. K. Laird¹, S. Lawlor¹, H. M. Lee², D. A. Leongamornlert¹, G. Laird¹, C. Lloyd¹, D. M. Lloyd¹, J. Loveland¹, J. Lovell¹, S. McLaren¹, K. E. McLay¹, A. McMurray¹, M. Mashreghi-Mohammadi¹, L. Matthews¹, S. Milne¹, T. Nickerson¹, M. Nguyen², E. Overton-Larty¹, S. A. Palmer¹, A. V. Pearce¹, A. I. Peck¹, S. Pelan¹, B. Phillimore¹, K. Porter¹, C. M. Rice¹, A. Rogosin^{2,3}, M. T. Ross¹, T. Sarafidou⁴, H. K. Sehra¹, R. Shownkeen¹, C. D. Skuce¹, M. Smith¹, L. Standing², N. Sycamore¹, J. Tester¹, A. Thorpe¹, W. Torcasso², A. Tracey¹, A. Tromans¹, J. Tsolas^{2,3}, M. Wall¹, J. Walsh², H. Wang², K. Weinstock², A. P. West¹, D. L. Willey¹, S. L. Whitehead¹, L. Wilming¹, P. W. Wray¹, L. Young¹, Y. Chen⁵, R. C. Lovering⁶, N. K. Moschonas⁴, R. Siebert⁷, K. Fichtel², D. Bentley¹, R. Durbin¹, T. Hubbard¹, L. Doucette-Stamm^{2,3}, S. Beck¹, D. R. Smith^{2,3} & J. Rogers¹

¹The Wellcome Trust Sanger Institute, Wellcome Trust Genome Campus, Hinxton CB10 1SA, UK

²Genome Therapeutics Corporation, 100 Beaver Street, Waltham, Massachusetts 02453, USA

³Agencourt Bioscience Corporation, 100 Cummings Center, Beverly, Massachusetts 01915, USA

⁴Department of Biology, University of Crete & Institute of Molecular Biology and Biotechnology, Foundation of Research and Technology, PO Box 2208, 71409 Heraklion, Crete, Greece

⁵European Bioinformatics Institute (EBI), Wellcome Trust Genome Campus, Hinxton CB10 1SD, UK

⁶HUGO Gene Nomenclature Committee, Department of Biology, University College London, London NW1 2HE, UK

⁷Institute of Human Genetics, University Hospital Schleswig-Holstein Campus Kiel, Schwanenweg 24, D-24105 Kiel, Germany

The finished sequence of human chromosome 10 comprises a total of 131,666,441 base pairs. It represents 99.4% of the euchromatic DNA and includes one megabase of heterochromatic sequence within the pericentromeric region of the short and long arm of the chromosome. Sequence annotation revealed 1,357 genes, of which 816 are protein coding, and 430 are pseudogenes. We observed widespread occurrence of overlapping coding genes (either strand) and identified 67 antisense transcripts. Our analysis suggests that both inter- and intrachromosomal segmental duplications have impacted on the gene count on chromosome 10. Multispecies comparative analysis indicated that we can readily annotate the protein-coding genes with current resources. We estimate that over 95% of all coding exons were identified in this study. Assessment of single base changes between the human chromosome 10 and chimpanzee sequence revealed nonsense mutations in only 21 coding genes with respect to the human sequence.

We report here the final clone map and sequence assembly of human chromosome 10. This metacentric chromosome accounts for 4.5% of the genome and is best known for harbouring the *PTEN* tumour suppressor gene and the *RET* proto-oncogene.

With the human genome sequence in hand, the task ahead is to identify the different units of genetic information embedded in the sequence and understand their function both at the molecular and cellular level. In this study we address the former by reporting a comprehensive annotation of manually inspected gene structures and their correlation to sequence variation and other features of the genomic sequence. The annotation process is assessed by comparative analysis to the genome sequence of two rodents, *Mus musculus* and *Rattus norvegicus*, and three fishes, *Tetraodon nigroviridis*, *Fugu rubripes* and *Danio rerio*. Finally, we report our preliminary findings on the distribution of single base differences along human chromosome 10 in comparison to the chimpanzee genome.

The clone map and finished sequence

A clone map spanning the euchromatic regions of the short (p) and long (q) arm of human chromosome 10 was assembled by restriction fingerprint and sequence-tagged site (STS) content analysis¹. We identified clones by screening approximately 85 genomic equivalents of P1-derived artificial chromosome (PAC), bacterial

artificial chromosome (BAC), yeast artificial chromosome (YAC), cosmid and fosmid libraries. The tiling path consists of 1,144 minimally overlapping clones (Supplementary Table S1) organized into 12 contigs (Table 1). Contig-1340 spans the entire p arm and harbours the boundary between euchromatin and heterochromatin with the proximal 250 kilobases (kb) extending into pericentromeric satellite repeats. In a detailed study of this region two further clones carrying satellite 3 sequences, contig-2069, were identified and mapped by pulse field gel electrophoresis (PFGE) ~50 kb proximal to contig-1340 (ref. 2). Similarly, contig-43 harbours the q-arm boundary with the proximal 240 kb composed of satellite repeats³. In addition, clone RP11-745D9, 94% of which consists of α -satellite repeats, was arbitrarily placed proximal to contig-43 as it was suggested to map to human chromosome 10 (E. Eichler, personal communication). A 9.75-megabase (Mb) PFGE map spanning the chromosome 10 centromere⁴ places the core α -satellite block (D10Z1) ~0.2 Mb distal to contig-102 and 1 Mb proximal to contig-43.

In contrast with the p arm, nine gaps remain in the clone map of the q arm. Five of them are clustered within a ~4-Mb region (Table 1 and Fig. 1 (rollfold); see also Supplementary Fig. S1 for a detailed view). Our inability to walk across these five gaps was due to the extensive segmental duplications in this region (Fig. 2);

however, we obtained a size estimate by fluorescent *in situ* hybridization (FISH) of RP11-172C24 (AL512595) and RP11-13E1 (AC013284) on metaphase chromosomes. We sized the remaining four gaps by FISH with clones immediately flanking each gap to extended DNA fibres. No gap was estimated to be larger than 50 kb in size. Altogether the euchromatic gaps account for no more than 840 kb (Table 1). Finally, we defined the location of both telomeres. Clone RP11-631M1 (AL713922) ends ~20 kb away from the telomeric repeats of the p arm based on the telomeric half-YAC XX-YAC22O3 (<http://www.wistar.upenn.edu/Riethman/>). At the end of the q arm (qtel), clone XX-YAC2136 (BX322534) contains part of the telomeric repeat block.

Each clone of the tiling path was subjected to random subcloning and sequencing at either the Genome Therapeutics Corporation (GENE) or the Sanger Institute—the initial draft sequence of a few clones was carried out by other centres that are credited in the corresponding submissions to the EMBL/GenBank/DBJ databases. We finished clones according to the international finishing standard (<http://genome.wustl.edu/Overview/g16stand.php>). Of the 1,144 clones in the human chromosome 10 tiling path, 221 and 913 were finished at GENE and the Sanger Institute, respectively, and three elsewhere (Supplementary Fig. S1). The remaining seven clones show persistent deletion of internal fragments. In total, we finished 131,666,441 base pairs (bp) in 18 sequence contigs; euchromatic coverage is estimated at 99.4%. Sequence accuracy was estimated as described in ref. 5 and found to exceed 99.99%. The sequence assembly comprises all known chromosome 10 messenger RNAs (RefSeq set) and STS markers from available radiation hybrid⁶ and genetic maps^{7,8} (T. Furey, personal communication). In addition, the integrity of the sequence map was independently assessed at the University of California, Santa Cruz, by alignment of fosmid and BAC paired end sequences (<http://genome.cse.ucsc.edu/>). Table 1 lists the size of each sequence contig, with the largest one spanning 44,693,577 bp.

Table 1 Clone and sequence contigs on chromosome 10

Clone contig	Sequence contig	Size (bp)	Gap size estimate (bp)
Telomere	—	—	20,000
1340	BX32259-BX276080	5,574,992	10,000
	AL365356-BX255924	12,337,510	10,000
	AL928729-AL133216	20,793,917	—
Gap	—	—	50,000
2069	AL133173-AL590623	286,100	—
Gap	—	—	50,000
Centromere	—	—	2,380,000
Gap	—	—	50,000
102	BX322613	191,752	—
Gap	—	—	50,000
43	AL031601-AC012044	3,830,268	—
Gap*	—	—	ND*
4000	AL831769-BX649215	952,201	—
Gap*	—	—	ND*
3003	AL450388-AL603965	263,307	—
Gap*	—	—	ND*
101	AL954360	163,321	—
Gap*	—	—	ND*
14	BX547991-AL731733	989,826	—
Gap*	—	—	ND*
15	AL603966-AL731572	1,941,839	10,000
	AL672187	211,435	10,000
	AL589822-AL132656	30,068,948	—
Gap	—	—	10,000
16	AC068139-AL731667	44,693,577	10,000
	AL606510-AL772134	2,696,534	—
Gap	—	—	50,000
17	BX470155-AL607044	4,615,046	—
Gap	—	—	10,000
2493 (includes telomere)	BX294094-BX511297	246,123	10,000
	AL732395-BX322534	1,809,745	—

*Cumulative gap size estimate of 750,000 for all five of the indicated gaps together. ND, not determined.

The gene and protein index

The Sanger Institute has established a standardized annotation pipeline (outlined at <http://vega.sanger.ac.uk/>) in which gene structures are drawn on the basis of human interpretation of the combined supportive evidence generated during sequence analysis. Annotation of the human chromosome 10 sequence resulted in a total of 1,787 gene structures that we then classified, as described in ref. 9, into: (1) 654 'known' genes; (2) 162 'novel genes'; (3) 219 'novel transcripts'; (4) 322 'putative genes'; and (5) 430 'pseudogenes'. Pseudogenes were further subdivided into processed (371) and unprocessed (59).

Excluding the pseudogenes, human chromosome 10 is a chromosome with an average gene density (10.4 genes Mb⁻¹). The 1,357 genes span 66,309,730 bp in total (mean 51,335 bp per gene). Therefore, 50.6% of the analysed sequence is transcribed, matching the figure reported for chromosome 22 (51%), which is gene-rich, but appearing elevated in comparison with chromosomes 6, 7, 14 and 20 (42.2%, 46.5%, 43.6% and 42.4%, respectively), which have gene densities similar to chromosome 10. The latter suggests that the human chromosome 10 genes have on average a larger genomic span than those on chromosomes 6, 7, 14 and 20. Gene size along human chromosome 10 varies enormously, with the two extremes being *CTNNA3* (1,776,209 bp) and *CALML5* (859 bp). Exons account for only 2.3% of the sequence and the mean exon size is 313 bp. The longest and shortest exons annotated in this study have a length of 9,763 (*SH3MD1*) and 3 bp (*CDH23*), respectively. *CDH23* is also the gene with most exons (69) on this chromosome. Table 2 summarizes the features of each gene class.

Alternative splicing is a major contributor to the complexity of the human transcriptome. We annotated a total of 4,204 transcripts for 1,357 gene structures (Table 2). No splice variants were annotated on the basis of alternative polyadenylation sites. Approximately 73% of the protein-coding genes have more than one transcript and 5.8 on average. For *ADD3* we annotated 22 variants. Note that the use of partial expressed sequences (for example, expressed sequence tags (ESTs)) may result in the annotation of more than one transcript per splice variant. Given this caveat, our analysis suggests a significantly higher level of alternative splicing compared with previous estimates¹⁰. Approximately 50% of the 3,456 transcripts (known and novel) do not seem to encode a protein. Annotation of these transcripts is largely based on ESTs, many of which may correspond to aberrant transcripts. Their precise role is largely unknown but they may be part of the machinery of transcriptional regulation (for example, via nonsense-mediated decay). Nevertheless, there are 1,837 transcripts with an open reading frame (ORF). Of the 342 genes with at least two transcripts having a complete ORF (that is, possess both a 5' and a 3' untranslated region (UTR)), 312 encode at least two distinct peptides.

Identification of transcription start sites and promoter regions remains a challenge in the annotation process. First, we scanned the human chromosome 10 unmasked sequence and predicted a total of

Figure 1 The sequence map of chromosome 10 and its features (see rollfold). The current sequence assembly (v1.1) and that used in the analysis presented in this study (v1.0) are available at <http://www.sanger.ac.uk/HGP/Chr10>. Tracks from top to bottom are: (1) the scale bar (in Mb); (2) the sequence map of human chromosome 10 represented by a black solid bar interrupted by clone and sequence gaps (grey); (3) syntenic blocks in the mouse (top track) and the rat (bottom track) where blocks are colour-coded per chromosome and labelled with the chromosome number and coordinates (Mb) (for example, 2: 3.1–11.3 Mb; unordered sequence contigs are tagged as random); (4) predicted CpG islands (brown); (5) regions of sequence homology to *Fugu* (blue), zebrafish (dark blue) and *Tetraodon* (dark pink); and (6) protein-coding genes. Gene names are in dark blue for the known and black for the novel CDS.

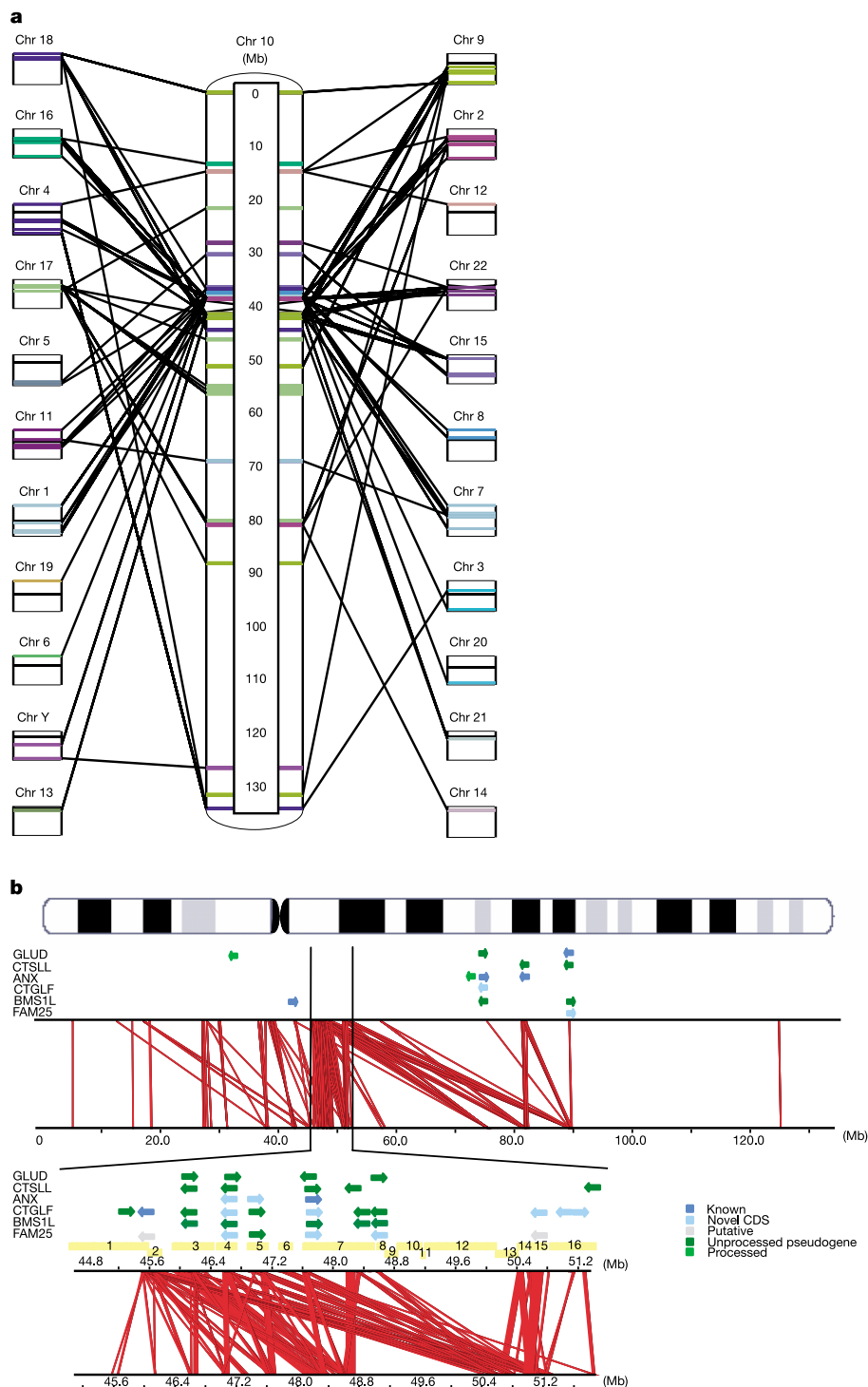


Figure 2 Chromosome 10 inter- and intrasegmental duplications. **a**, Interchromosomal duplications across chromosome 10 showing blocks of 10 kb or greater. Duplicated regions are colour-coded per chromosome and indicated as lines (thickness is proportional to physical distance). Each chromosome other than 10 is represented by an open black rectangle with a black line representing the centromere. **b**, 10q11:10q22:10q23.1:10q23.3 intrasegmental duplications. Top row, ideogram of chromosome 10; second row, positions of members of the six main gene families outside 10q11 (colour-coded per gene class; arrows indicate transcription); third row, intrachromosomal duplications across the whole chromosome showing blocks of 10 kb or greater; bottom row, enlarged view of the 10q11 region. Yellow bars represent sequence (bottom row for sequences submitted in reverse orientation) contigs between AL358394 and AL589794 (complete clone list in Supplementary Fig. S1). From left to right the

members (where parentheses indicate members only appearing in the enlarged section) of each family are: GLUD family, *GLUDP5*, (*GLUDP7*, *GLUDP8*, *GLUDP6*, *GLUDP2*), *GLUDP3*, *GLUD1*; CTSLL family, (*CTSLL5*, *CTSLL7*, *CTSLL2*, *CTSLL3*, *CTSLL4*), *CTSLL6*, *CTSLL1*; ANXA family, (*ANXA8L1*, *ANXA8L2*, *ANXA8*), *ANXA2P3*, *ANXA7*, *ANXA11*; CTGLF family, (*CTGLF10P*, *CTGLF1*, *CTGLF13P*, *CTGLF7*, *CTGLF11P*, *CTGLF6*, *CTGLF9P*, *CTGLF12P*, *CTGLF5*, *CTGLF4*, *CTGLF3*), *CTGLF2*; BMS1L family, *BMS1L*, (*BMSILP1*, *BMSILP2*, *BMSILP6*, *BMSILP5*, *BMSILP7*), *BMSILP4*, *BMSILP3*; FAM25 family, (*FAM25E*, *FAM25B*, *FAM25HP*, *FAM25G*, *FAM25C*, *FAM25D*), *FAM25A*. *ANXA7* and *ANXA11* were included owing to their proximity to the 10q22 and 10q23.1 locus, respectively. Seven *CTGLF1* paralogues (Supplementary Table S3) were annotated as novel genes for consistency but probably represent expressed pseudogenes.

Table 2 Structural characteristics of annotated gene structures on chromosome 10

Gene structure class	Number of genes	Total transcribed length (bp)	Mean gene length (bp)	Mean exon length (bp)	Mean transcripts per gene	Mean exons per gene
Known genes	654	56,312,218	86,870	316	4.76	11.02
Novel CDS	162	3,615,155	22,435	344	2.12	4.96
Total protein coding	816	59,482,121	74,078	320	4.24	9.81
Novel transcript	219	6,123,588	29,166	272	1.77	4.06
Putative genes	322	2,798,239	8,780	287	1.12	2.15
Processed pseudogenes	371	328,131	887	638	1.00	1.19
Unprocessed	59	982,662	16,655	176	1.00	6.95
Total structures	1,787	67,353,917	39,717	322	2.59	5.84

Note that transcribed length is not additive because some genes overlap. CDS, coding sequence.

1,025 CpG islands (Fig. 1), which are known to be associated with the 5' end of an estimated 60% of human genes¹¹. We then used Eponine¹² to predict transcription start sites and FirstEF¹³ to predict regions that encompass the promoter and 5' exon. In total, FirstEF and Eponine predicted 1,801 (rank = 1, score ≥0.8) and 2,800 features, respectively (Supplementary Fig. S1). Notably, 62% of FirstEF and 96% of Eponine features directly overlapped CpG islands, suggesting a heavy bias towards this feature in both algorithms. The distribution of CpG islands, FirstEF and Eponine hits was also assessed relative to the first exon of each of the 4,635 annotated transcripts using a window of 5,000 bp upstream and 1,000 bp downstream of the exon. Table 3 summarizes the results obtained per gene class. For example, in the 'known' class, 1,544 (49.6%) and 1,124 (36.1%) transcripts had a FirstEF and Eponine feature, respectively. Not surprisingly, 89.9% of FirstEF and 96.7% of Eponine transcripts were also associated with a CpG island. Note that Eponine predicts multiple transcription start sites per transcript (4.24 on average).

Regulation of gene expression by antisense transcription is a recognized mechanism with examples reported in species ranging from bacteria to mammals^{14–16}. We observed widespread occurrence of overlapping coding genes (either strand) in human chromosome 10 (101 pairs in total). In 38 cases one of the genes is fully contained within an intron of the other, typically on the opposite strand (34). For example, the second intron of the splice variant LIPA-004 encompasses four members of the IFIT gene cluster (Supplementary Table S3 and Fig. S2) and appears to be transcribed from the same bidirectional promoter as *IFIT5* (IFIT cluster member). Interestingly, the LIPA-001 and -002 variants do not overlap any IFIT gene, whereas LIPA-003 and LIPA-005 both overlap with *IFIT2* and *IFIT4* (Supplementary Fig. S2). Mutations in *LIPA* can cause Wolman and cholesteryl ester storage disease (Online Mendelian Inheritance in Man (OMIM) 278000). Among partially overlapping pairs (opposite strands), 34% involve the respective 5' exons, which is indicative in each case of a bidirectional promoter. We also searched for non-coding transcripts located on the opposite strand of coding genes. There are 67 antisense transcripts overlapping 63 coding genes. The two most common patterns observed were intragenic with partial overlap of one exon, and partial overlap with the most 5' exon of the coding gene. For *ZNF32*, we found two antisense transcripts (*ZNF32OS1* and *ZNF32OS2*).

Finally, we looked at the distribution of known protein domains

in both human chromosome 10 (this study) and the whole genome (Ensembl v.17.33.1) proteome using InterProScan. At the gene level, 70.6% of the human chromosome 10 peptides have at least one InterPro match with a Pfam domain and 32% are multidomain (1.37 distinct InterPros on average). Supplementary Table S2 shows the top 24 domains in chromosome 10 alongside their genome-wide ranking, suggesting that this chromosome is enriched in peptides with a lipase (IPR000734), aldo/keto reductase (IPR001395) or alpha/beta hydrolase (IPR000073) domain. BLASTP analysis (*e*-values <10⁻¹⁵) showed that all six genes encoding the peptides carrying the IPR001395 domain are clustered (AKRIC cluster) at position 4.8–5.3 Mb, whereas there are two lipase clusters, LIP (90.0–91.0 Mb; six members) and PNLIP (117.9–118.1 Mb; four members). In total, we found 42 gene clusters along human chromosome 10 (Supplementary Table S3).

Genomic landscape

The average G+C and repeat content of human chromosome 10 are 41.58% and 43.66%, respectively. The distribution of the main classes of repeats (Supplementary Table S4), the G+C and CpG density plots all seem to follow the known genome-wide trends. For example, the G+C content fluctuates along the chromosome, peaks at the qtel and is positively correlated to gene density (Supplementary Fig. S1). Large genes tend to be located adjacent to or within gene-poor regions, for example *PRKG1* and *PCDH15* (interval 52.0–59.0 Mb), whereas regions of high gene density seem enriched in short interspersed elements (SINES).

Segmental duplications are an important feature of the genomic landscape, being an integral part of the evolutionary machinery. Figure 2a illustrates the interchromosomal duplications along human chromosome 10 (see also ref. 17 and <http://humanparalogy.cwru.edu/SDD>). Figure 2b shows the extensive segmental duplications within a 5 Mb region at 10q11 with sequences further dispersed at 10q22, 10q23.1 and 10q23.2. Using the draft genome sequence Crosier and colleagues¹⁸ reported that 10q11 has been subject to multiple rounds of local duplications in at least the last 30–40 million years (Myr); they also showed that a 10q11:10q23 paracentric inversion occurred after the divergence of orang-utan from other great apes and hypothesized that the 10q22 locus resulted from chromosome-specific duplicative transposition. Bryce and colleagues¹⁹ characterized three cathepsin-L-like paralogues, which are expressed pseudogenes, and reported FISH signals

Table 3 Correlation of CpG island, FirstEF and Eponine features with annotated transcripts

Gene class	All Transcripts		FirstEF transcripts		Eponine transcripts	
	Complete	Incomplete	Complete	Incomplete	Complete	Incomplete
Known	1,490 (580)	1,623 (1,018)	593 (531)	951 (877)	421 (412)	703 (682)
Novel CDS	130 (57)	213 (75)	45 (43)	62 (57)	38 (38)	43 (41)
Novel transcript	388 (119)	0 (0)	120 (105)	0 (0)	83 (79)	0 (0)
Processed pseudogene	371 (32)	0 (0)	29 (22)	0 (0)	21 (19)	0 (0)
Unprocessed pseudogene	59 (11)	1 (2)	14 (10)	1 (1)	9 (8)	0 (0)
Putative	360 (74)	0 (0)	87 (64)	0 (0)	57 (50)	0 (0)

Values in parentheses are for transcripts associated with a CpG island.

at 10q11, 10q22 and 10q23, a pattern previously seen with the *GLUD* paralogues²⁰ (Fig. 2b). The duplication of the *CTSL* locus between chromosomes 9 and 10 was estimated to have occurred some 40 Myr ago¹⁹. We identified four and three additional *CTSL* and *GLUD* pseudogenes, respectively (Fig. 2b), consistent with the local duplication events involving *BMS1L* (known as *KIAA0187*)¹⁸ and *CTGLF1* (this study). In total, we annotated 7 *BMS1L* and 11 *CTGLF1* paralogues (Fig. 2b; functional genes in dark blue). Retro-position of a truncated *KIAA1099* (*CENTG2*; chromosome 2) mRNA gave rise to a processed pseudogene on chromosome 10 (ref. 18). However, this pseudogene forms the 3' exon of *CTGLF1*, suggesting that this gene resulted from a fusion between an ancestral gene and the *CENTG2* pseudogene, and the retroposition event predated all segmental duplications. Note that there is also evidence of transcripts combining exons of *CTGLF1* and *BMS1L* paralogues. Interestingly, we predicted a novel gene, *FAM25A* (based on mouse complementary DNA AK008614 and without similarity to any known protein), with seven human chromosome 10 paralogues (Fig. 2b) that follow the pattern of *GLUD*, *BMS1L*, *CTGLF* and *CTSL*. In addition to these five types of low copy repeats, the segmental duplications in 10q11:10q22:10q23 seem to have impacted on the number of genes on this chromosome. Notably, 31% of all the functionally related gene clusters are located within 10q11 and 10q23 (Supplementary Fig. S1 and Table S3).

The average recombination rate across the chromosome is 1.32 cM Mb⁻¹ (Fig. 3, sex average). Note that ref. 7 used the draft human chromosome 10 sequence (inflated by ~8%) and thus obtained a lower figure (1.21 cM Mb⁻¹). The rate of male recombination is higher than the female rate near the telomeres, whereas between D10S211 and D10S575 the female rate is higher (Fig. 3). This comparison also indicates the presence of two female-specific recombination hotspots (Fig. 3, arrows). As expected, pericentromeric regions display a low rate of recombination, more than twofold below the chromosome average. In particular, the region between D10S1247 and D10S1783 has a rate of 0.3 cM Mb⁻¹ and contains the only human chromosome 10 recombination 'desert'²¹. The region of extensive segmental duplications at 10q11 shows a low

rate of recombination (0.72 cM Mb⁻¹). Thus, meiotic recombination is unlikely to have been the driving force in generating these duplications. Our analysis confirmed the recombination 'jungle' between D10S1782–D10S1651, which we extended to D10S212 (3.4 cM Mb⁻¹); we refuted the one between D10S189 and D10S1728 (2.3 cM Mb⁻¹), and identified a new one between D10S1154 and D10S552 (4.55 cM Mb⁻¹).

Comparative sequence analysis

Many of the functional units in present-day vertebrate genomes have been conserved through evolution. Coding regions are highly conserved across all vertebrates, whereas non-coding regions are conserved among more closely related species. The genome sequences of three fishes (*Tetraodon*, *Fugu* and zebrafish) and two rodents (mouse and rat) were publicly available at the time of analysis. We compared the sequence of human chromosome 10 to each of the above species and searched for conserved regions with coding potential—distinguishing functional non-coding elements above background sequence conservation requires the use of additional genomes²². We then correlated the obtained hits in each species with the annotated genes. As expected, each of the fish genomes showed higher specificity (>0.82; that is, 82% of sequences conserved in fish overlapped human annotated exons) than the rodents (>0.29), whereas the highest specificity was obtained using all genomes together (0.96). Sensitivity was higher using a rodent genome (0.7; that is, 70% of all annotated exons had matches in rodent) than a fish genome (0.4).

Of the 1,787 gene structures (16,765 exons), 84% (78% of exons) had at least one exon supported by a conserved region in one of the other genomes and 52% (32% of exons) in all genomes. Note that the figures given for exons are underestimated owing to lower sequence conservation in the untranslated regions. Protein-coding genes are highly conserved (98.5%; 85% of exons). In contrast, 61% (29% of exons) and 45% (27% of exons) of novel transcripts and putative genes, respectively, have at least one match. Furthermore, only 21% of novel transcripts and 8% of putative genes show conservation with a fish (91% for protein-coding genes). Typically, novel transcripts were annotated on the basis of solid experimental evidence (that is, human mRNA) and may represent either genes that have evolved more rapidly or non-coding RNAs.

On the basis of specificity, regions conserved in all six species can serve as a measure of completeness of the gene annotation process that occurred independently of the comparative analysis. We found 5,604 such evolutionarily conserved regions (ECRs) of which 5,292 mapped inside annotated exons (including pseudogenes). Of the remaining 312 ECRs, 142 were intergenic and 170 intragenic. On inspection, we found 79 of these ECRs with supportive evidence to annotate a missed exon, most of which were part of a pseudogene (79%). The remaining 233 ECRs provide the basis to estimate that we have annotated at least 95.8% of all conserved coding exons on human chromosome 10. This is a conservative estimate as 131 of these ECRs are located in introns and may represent conserved non-exonic sequences. Interestingly, 54 (41%) of them are associated with just four genes: *C10orf11* (26; also known as *CDA017*), *EBF3* (20), *TCF7L2* (5) and *PAX2* (3). All but *C10orf11* (unknown function) are transcription factors. Figure 4 shows a MultiPip-Maker²³ alignment of the orthologous *EBF3* loci and the relative position of ECRs in the human gene. Note that sequence identity is often higher in ECRs than in exons.

Sequence variation

During the human chromosome 10 project we discovered 35,882 single nucleotide polymorphisms (SNPs) by sequence alignment in regions of clone overlaps. In total, we mapped 143,364 SNPs (dbSNP release 115) to the chromosome 10 sequence. Supplementary Fig. S1 shows the density plots for randomly discovered²⁴ and all SNPs across the chromosome.

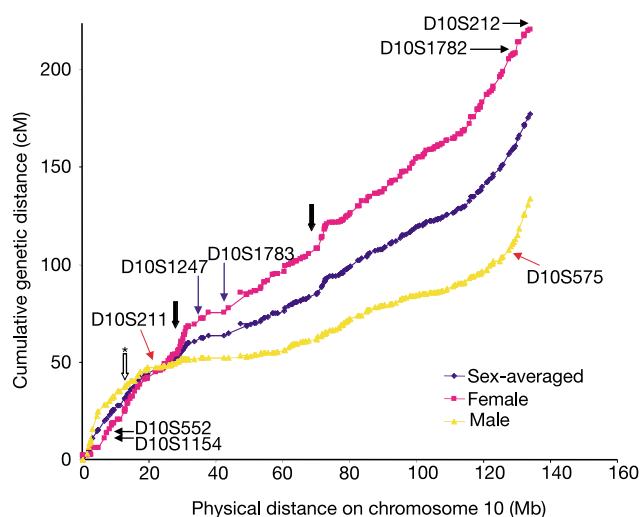


Figure 3 Alignment of the deCODE genetic map of chromosome 10 to the physical map from the telomeric end of the short arm to the telomeric end of the long arm. The position of each genetic marker on the female, male and sex-averaged genetic map is indicated. Female-specific recombination hotspots are indicated by thick arrows (left, D10S1732–D10S208; right, D10S599–D10S676). The location of markers flanking recombination deserts (blue arrows) and jungles (black arrows) is shown. The asterisk indicates the location of the refuted jungle (D10S189–D10S1728).

There are 5,864 (4.1%) exonic and 65,973 (46%) intronic SNPs. Of the 1,821 SNPs in coding exons 984 are non-synonymous. *MSMB* has the most polymorphic coding region with 43 SNPs kb⁻¹; it encodes a protein with inhibin-like activity and its expression is decreased in prostate cancer²⁵.

We also considered 729,553 human–chimpanzee single base differences (SBDs) remapped on the current assembly of human chromosome 10. These were high-confidence sequence differences originally identified by aligning 14 million shotgun reads of the chimpanzee genome, generated jointly by the Whitehead Institute and Washington University Genome Centers, to the human genome sequence assembly (NCBI build 31). We first removed all human–chimpanzee SBDs that co-localized with known human SNPs. Supplementary Fig. S1 shows the density plot of the remaining 703,338 SBDs. Of those, 55.3% are intergenic, 42.9% intronic and 1.8% exonic. The highest density of human–chimpanzee SBDs, fourfold greater than the average level, was observed in a 200-kb gene-poor region at 19.43–19.63 Mb. We then examined the 12,710 human–chimpanzee SBDs that lie in exons of the 816 human coding genes. Of those, 3,972 were in coding regions and can be subdivided further into 2,273 synonymous, 1,678 non-synonymous and 21 nonsense with respect to the human sequence. For each gene we calculated the rate of evolution of non-synonymous (K_a) and synonymous (K_s) changes, and the ratio K_a/K_s , which provides a measure of evolutionary selection. Supplementary Table S5 lists the 1,413 transcripts with at least one coding human–chimpanzee SBD sorted on the K_a/K_s value. There are only 29 transcripts (21 genes) that have a K_a/K_s value ≥ 1 , whereas there are 484 without non-synonymous SBDs. Note that several caveats apply in this type of analysis owing to the incomplete nature of both the chimpanzee data and the list of human SNPs; we used the number of intronic human–chimpanzee SBDs per base in comparison to the chromosome average of 0.005 as a possible estimate of coverage. The gene with most non-synonymous human–chimpanzee SBDs is *MKI67*, an antigen identified by monoclonal antibody Ki-67, which appears to be fast evolving in humans ($K_a/K_s = 1.038507$; SNP data). The expression pattern of *MKI67* in gastric and other cancers is under investigation as this gene is expressed in proliferating cells. Interestingly, a nonsense human–chimpanzee SBD is present in both of its coding transcripts. Among the 21 genes with nonsense human–chimpanzee SBDs notable examples are the serotonin receptor *HTR7* (the neurotransmitter serotonin is thought to be involved

in cognition and behaviour), *PSAP* (prosaposin; involved in variant Gaucher's disease and metachromatic leukodystrophy) and the developmental gene *NODAL*.

Medical implications

At the time of writing there were 85 disease loci reported on human chromosome 10 (<http://www.ncbi.nlm.nih.gov/omim/>), a 47% increase since 1999 (ref. 26). Several of these loci account for multiple disease phenotypes caused by mutations in the same gene; notable examples are *FGFR2* (OMIM 176943), *PTEN* (OMIM 601728) and the proto-oncogene *RET* (OMIM 164761). Since *PTEN* was first shown to be mutated in brain, breast and prostate cancers²⁷, there has been an explosion of reported mutations (110 germline and 332 somatic mutations)²⁸ and disease phenotypes²⁹. Human chromosome 10 harbours several other genes involved in tumorigenesis; for example, deregulation of *TLX1*, *NFKB2* or *BMI1* caused by chromosomal translocations or amplifications has been detected in lymphatic neoplasms. Mapping of allelic imbalances and functional studies suggest the presence of additional tumour-related genes. The finished and annotated sequence is key in the process of cloning these and other hitherto unidentified disease-associated genes.

The prompt release of both the clone and sequence map resources throughout the project has accelerated the cloning of many disease-causing genes. To this end we recently showed as part of the European ADLTE consortium that mutations in the *LGII* gene cause autosomal dominant lateral temporal epilepsy³⁰. Notably, we found that the *FRA10A* folate-sensitive fragile site is located close to *LGII* and its expression is associated with the expansion of a polymorphic CGG repeat located at the 5' UTR of *FRA10AC1*, a gene encoding a novel nuclear protein³¹. There are seven fragile sites mapping to human chromosome 10 (ref. 32).

The challenge ahead is to unravel the molecular basis of common disease. An increasing number of susceptibility loci for complex diseases is being mapped to human chromosome 10, including metabolic diseases such as type I diabetes (IDDM10 and IDDM17), psychiatric disorders such as schizophrenia, or neurodegenerative illnesses such as Alzheimer's disease^{26,32}. In a case control study of morbidly obese and healthy individuals Boutin and colleagues³³ identified a SNP in the *GAD2* gene that increases the risk for obesity as well as a protective haplotype. Studies so far have mainly focused on candidate genes. The construction of a comprehensive haplotype

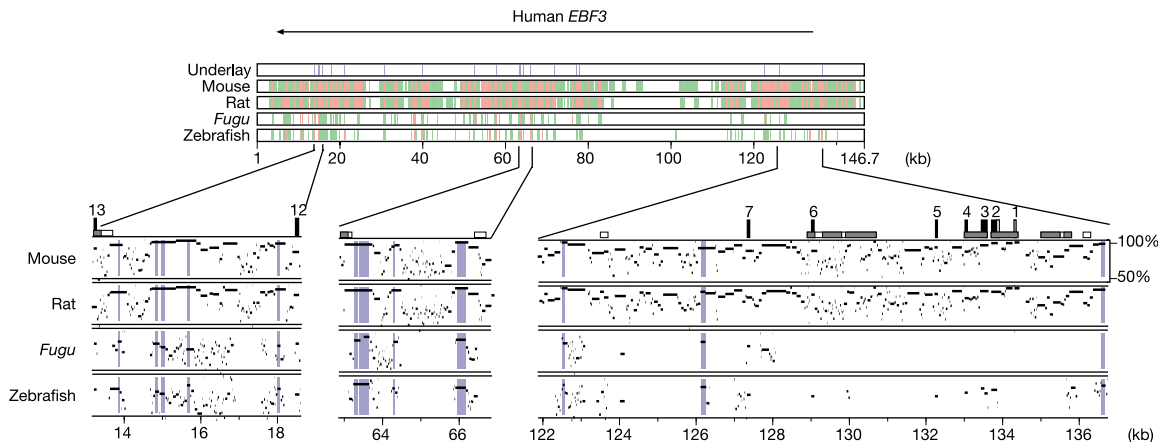


Figure 4 Multispecies alignment of orthologous *EBF3* loci. The human early B-cell factor 3 (*EBF3*) gene is represented by the arrow at the top. Alignments are displayed using MultiPipMaker²³. In the top panel, the first track shows the location of the ECRs (blue lines) across the human locus, whereas the following four tracks show regions conserved in mouse, rat, *Fugu* and zebrafish, respectively (green, aligned regions; orange, aligned

regions with at least 70% nucleotide identity and no gap over 100 bp). The bottom panel shows a detailed view of the three regions with the highest number of ECRs. Vertical black and grey numbered boxes represent coding and UTR exons, respectively. The scale at the right indicates the percentage of sequence identity. Physical distance is given in kilobases (kb).

map of the human genome is well underway³⁴, making it possible to undertake a systematic approach to scanning the genome for associations to disease-related and other phenotypes. □

Methods

The mapping and sequencing methods used in the assembly of the bacterial clone and sequence map of chromosome 10, respectively, as well as the tools of the gene annotation pipeline are described in refs 1 and 35 (see ref. 36 for detailed protocols). Manual annotation of gene structures followed the guidelines agreed in the human annotation workshop (HAWK; <http://www.sanger.ac.uk/HGP/havana/hawk.shtml>), whereas gene symbols were approved where possible by the HUGO Gene Nomenclature Committee³⁷. Protein translations were analysed with InterProScan (<http://www.ebi.ac.uk/interpro/scan.html>), which was run via the Ensembl protein annotation pipeline, to obtain Pfam, Prosite, Prints and Profiles domain matches.

Alignments for inter- and intrachromosomal duplications were performed with WU-BLASTN (<http://blast.wustl.edu>) using the current sequence assembly of chromosome 10 and the NCBI34 build for the rest of the genome. All sequences were repeat masked with RepeatMasker (<http://repeatmasker.genome.washington.edu>) and low-quality alignments (*e*-value > 10⁻³⁰, sequence identity < 90%, length < 80 bp) were discarded. For intrachromosomal duplications, self matches were discarded. For interchromosomal duplications, the sequence was split into 400-kb segments. Adjacent matches in the same orientation were joined together as described by ref. 38. Only blocks of 10 kb or greater were retained.

The following sequence assemblies were used for comparative analysis: *M. musculus* NCBI build 30 (Mouse Genome Sequencing Consortium; http://www.ensembl.org/Mus_musculus/resources.html); *R. norvegicus* version 2.0 (Rat Genome Sequencing Consortium; <http://www.hgsc.bcm.tmc.edu/projects/rat>); *D. rerio* Assembly version 1 (Sanger Institute; http://www.sanger.ac.uk/Projects/D_rerio); *F. rubripes* version 2 (International Fugu Genome Consortium; <http://www.fugu-sg.org/project/info.html>); and *T. nigroviridis* version 6 (Genoscope and Whitehead Institute for Genome Research; <http://www.genoscope.cns.fr/externe/tetraodon/Ressource.html>). The repeat-masked sequence of chromosome 10 was aligned to the mouse and rat genome sequences using BLASTZ³⁹ and the resulting matches were post-processed by axtBest and subsetAxt (W. J. Kent; <http://www.soe.ucsc.edu/~kent/src>) as described elsewhere³⁵. Alignment of the three fish genome sequences to chromosome 10 was performed with WU-TBLASTX using the scoring matrix, parameters and filtering strategy applied by Exofish⁴⁰. Overlapping alignments to different sequences were merged to produce contiguous regions of sequence conservation, analogous to the ECRs or 'Ecores', reported by Exofish.

SNPs in sequence overlaps were identified using a modification of the SSAHA software⁴¹. The chromosome 10 SNPs (dbSNP release 115) were mapped to the sequence assembly of this chromosome (this study) first with SSAHA and then Cross-Match. Of the approximately 14 million chimpanzee reads (<http://www.genome.gov/11008056>) mapped onto the human sequence assembly (NCBI build 31), those mapping to chromosome 10 were remapped to our sequence assembly and used to identify human-chimpanzee SBDs.

Received 17 December 2003; accepted 9 March 2004; doi:10.1038/nature02462.

1. Bentley, D. R. *et al.* The physical maps for sequencing human chromosomes 1, 6, 9, 10, 13, 20 and X. *Nature* **409**, 942–943 (2001).
2. Guy, J. *et al.* Genomic sequence and transcriptional profile of the boundary between pericentromeric satellites and genes on human chromosome arm 10p. *Genome Res.* **13**, 159–172 (2003).
3. Guy, J. *et al.* Genomic sequence and transcriptional profile of the boundary between pericentromeric satellites and genes on human chromosome arm 10q. *Hum. Mol. Genet.* **9**, 2029–2042 (2000).
4. Jackson, M. S., See, C. G., Mulligan, L. M. & Lauffart, B. F. A 9.75-Mb map across the centromere of human chromosome 10. *Genomics* **33**, 258–270 (1996).
5. Felsenfeld, A., Peterson, J., Schloss, J. & Guyer, M. Assessing the quality of the DNA sequence from the Human Genome Project. *Genome Res.* **9**, 1–4 (1999).
6. Deloukas, P. *et al.* A physical map of 30,000 human genes. *Science* **282**, 744–746 (1998).
7. Kong, A. *et al.* A high-resolution recombination map of the human genome. *Nature Genet.* **31**, 241–247 (2002).
8. Broman, K. W., Murray, J. C., Sheffield, V. C., White, R. L. & Weber, J. L. Comprehensive human genetic maps: individual and sex-specific variation in recombination. *Am. J. Hum. Genet.* **63**, 861–869 (1998).
9. Deloukas, P. *et al.* The DNA sequence and comparative analysis of human chromosome 20. *Nature* **414**, 865–871 (2001).
10. International Human Genome Sequencing Consortium, Initial sequencing and analysis of the human genome. *Nature* **409**, 860–921 (2001).
11. Antequera, F. & Bird, A. Number of CpG islands and genes in human and mouse. *Proc. Natl Acad. Sci. USA* **90**, 11995–11999 (1993).
12. Down, T. A. & Hubbard, T. J. Computational detection and location of transcription start sites in mammalian genomic DNA. *Genome Res.* **12**, 458–461 (2002).
13. Davuluri, R. V., Grosse, I. & Zhang, M. Q. Computational identification of promoters and first exons in the human genome. *Nature Genet.* **29**, 412–417 (2001).

14. Wagner, E. G. & Simons, R. W. Antisense RNA control in bacteria, phages, and plasmids. *Annu. Rev. Microbiol.* **48**, 713–742 (1994).
15. Eddy, S. R. Non-coding RNA genes and the modern RNA world. *Nature Rev. Genet.* **2**, 919–929 (2001).
16. Kiyosawa, H. *et al.* Antisense transcripts with FANTOM2 clone set and their implications for gene regulation. *Genome Res.* **13**, 1324–1334 (2003).
17. Bailey, J. A. *et al.* Recent segmental duplications in the human genome. *Science* **297**, 1003–1007 (2002).
18. Crosier, M. *et al.* Human paralogs of KIAA0187 were created through independent pericentromeric-directed and chromosome-specific duplication mechanisms. *Genome Res.* **12**, 67–80 (2002).
19. Bryce, S. D. *et al.* A novel family of cathepsin L-like (CTSLL) sequences on human chromosome 10q and related transcripts. *Genomics* **24**, 568–576 (1994).
20. Deloukas, P., Dauwerse, J. G., Moschonas, N. K., van Ommen, G. J. & van Loon, A. P. Three human glutamate dehydrogenase genes (GLUD1, GLUDP2, and GLUDP3) are located on chromosome 10q, but are not closely physically linked. *Genomics* **17**, 676–681 (1993).
21. Yu, A. *et al.* Comparison of human genetic and sequence-based physical maps. *Nature* **409**, 951–953 (2001).
22. Thomas, J. W. *et al.* Comparative analyses of multi-species sequences from targeted genomic regions. *Nature* **424**, 788–793 (2003).
23. Schwartz, S. *et al.* PipMaker—a web server for aligning two genomic DNA sequences. *Genome Res.* **10**, 577–586 (2000).
24. Sachidanandam, R. *et al.* A map of human genome sequence variation containing 1.42 million single nucleotide polymorphisms. *Nature* **409**, 928–933 (2001).
25. Vanaja, D. K., Chevill, J. C., Iturria, S. J. & Young, C. Y. Transcriptional silencing of zinc finger protein 185 identified by expression profiling is associated with prostate cancer progression. *Cancer Res.* **63**, 3877–3882 (2003).
26. Deloukas, P., French, L., Meitinger, T. & Moschonas, N. K. Report of the third international workshop on human chromosome 10 mapping and sequencing 1999. *Cytogenet. Cell Genet.* **90**, 1–12 (2000).
27. Li, J. *et al.* PTEN, a putative protein tyrosine phosphatase gene mutated in human brain, breast, and prostate cancer. *Science* **275**, 1943–1946 (1997).
28. Bonneau, D. & Longy, M. Mutations of the human PTEN gene. *Hum. Mutat.* **16**, 109–122 (2000).
29. Eng, C. PTEN: one gene, many syndromes. *Hum. Mutat.* **22**, 183–198 (2003).
30. Morante-Redolat, J. M. *et al.* Mutations in the LGI1/Epitempin gene on 10q24 cause autosomal dominant lateral temporal epilepsy. *Hum. Mol. Genet.* **11**, 1119–1128 (2002).
31. Sarafidou, T. *et al.* Folate-sensitive fragile site *FRA10A* is due to an expansion of a CGG-repeat in a novel gene *FRA10AC1*, encoding a nuclear protein. *Genomics* (in the press).
32. Moschonas, N. K. in *Encyclopedia of the Human Genome* Vol. 1, 618–625 (Nature Publishing Group, London, 2003).
33. Boutin, P. *et al.* *GAD2* on chromosome 10p12 is a candidate gene for human obesity. *PLoS Biol.* **1**, 1–11 (2003).
34. The International HapMap Consortium. The International HapMap project. *Nature* **426**, 789–796 (2003).
35. Mungall, A. J. *et al.* The DNA sequence and analysis of human chromosome 6. *Nature* **425**, 805–811 (2003).
36. Dunham, I. (ed.) *Genome Mapping and Sequencing* (Horizon Scientific, Wymondham, UK).
37. Wain, H. M., Lush, M., Ducluzeau, F. & Povey, S. Genew: the human gene nomenclature database. *Nucleic Acids Res.* **30**, 169–171 (2002).
38. Cheung, J. *et al.* Genome-wide detection of segmental duplications and potential assembly errors in the human genome sequence. *Genome Biol.* **4**, R25 (2003).
39. Schwartz, S. *et al.* Human–mouse alignments with BLASTZ. *Genome Res.* **13**, 103–107 (2003).
40. Roest Crollius, H. *et al.* Estimate of human gene number provided by genome-wide analysis using *Tetraodon nigroviridis* DNA sequence. *Nature Genet.* **25**, 235–238 (2000).
41. Ning, Z., Cox, A. J. & Mullikin, J. C. SSAHA: a fast search method for large DNA databases. *Genome Res.* **11**, 1725–1729 (2001).

Supplementary Information accompanies the paper on www.nature.com/nature.

Acknowledgements We thank the *Fugu*, Mouse and Rat Genome Sequencing Consortia; Genoscope and Whitehead Institute for Genome Research (*Tetraodon* genome data); the members of the zebrafish project at the Sanger Institute; the groups at the Washington University Genome Sequencing Center and the Whitehead Institute for early access to the chimpanzee whole-genome shotgun data; the laboratories of H. Riethman and M. S. Jackson for the provision of telomeric and pericentromeric clones, respectively; H. M. Wain, E. A. Bruford, C. C. Talbot, V. K. Khodiyar, M. J. Lush, M. W. Wright and S. Povey for assigning official gene symbols; the EMBL, GenBank and Ensembl database groups; I. Dunham for critical reading of the manuscript; and the Wellcome Trust for financial support.

Competing interests statement The authors declare that they have no competing financial interests.

Correspondence and requests for materials should be addressed to P.D. (panos@sanger.ac.uk). All DNA sequences reported in this study have been deposited in the EMBL or GenBank databases and the accession numbers can be found in Supplementary Fig. S1.